JOURNAL OF MATERIALS SCIENCE 39 (2004) 6993–7001

Effects of minor additions on microstructure and creep performance of RR2086 SX superalloys

Y. H. KONG, Q. Z. CHEN*
Department of Mechanical Engineering, The University of Hong Kong, Pokfulam Road, Hong Kong
E-mail: qzchena@hkucc.hku.hk

D. M. KNOWLES
Materials Performance Technologies, P.O. Box 31310, Lower Hutt, New Zealand

A comparative investigation of creep performance in an experimental single crystal base alloy (designated RR2086) and modified (with additions of carbon, boron and hafnium) RR2086 superalloys has been undertaken. The alloys were creep tested over a temperature range of 850–1050°C. At 850°C/430 MPa, the creep behaviour of the modified alloy was slightly better than the base material, particularly in the tertiary creep stage. But at both 950°C/210 MPa and 1050°C/165 MPa, the creep strain of the modified alloy evolved more rapidly, resulting in a shorter creep life than the base RR2086. Microstructure investigation showed that the interdendritic regions of modified RR2086 contained relatively large, irregular γ' particles which rafted to a limited level during creep, and that the amount of pores was significantly reduced in the modified alloy owing to MC carbide formation. Analysis of the correlation between microstructure and creep performance revealed that the reduction of pores in the modified alloy was beneficial to creep behaviour at the tertiary stage, and resulted in a longer creep life in the modified alloy than in the base RR2086 at 850°C/430 MPa. However, large, irregular and partially rafted γ' particles and brittle MC phase in the interdendritic regions of the modified RR2086 caused a higher creep rate during the primary and secondary creep stages. The detrimental effect increased with creep temperature, counteracting the beneficial effect of porosity reduction. As a result the modified alloy had a shorter creep life than the base alloy at 950 and 1050°C.

1. Introduction

Single crystal (SX) superalloys have been successfully applied in the production of turbine blades. In SX blades there is no need for grain boundary strengthening elements such as carbon, boron, zirconium and hafnium [1, 2]. In fact, these elements are detrimental because they reduce the incipient melting temperature at which some components of the alloy melt [3]. However in the production of nozzle guide vanes, due to their complex shape, grain boundaries are difficult to avoid in attempting an SX casting process. In such cases where stray grains may form it has been suggested that the addition of C, B and Hf may have some benefit in that precipitation of grain boundary precipitates may lead to strengthening of the boundary.

The formation of carbides at grain boundaries is desirable to improved creep strength. However, carbides also appear in the matrix, which may affect other phase transformations, such as topologically close-packed (TCP) phase transformation. In previous work [4], it was found that a number of factors contributed to the creep performance of the modified RR2072 alloys, including MC carbides, TCP phase, porosity, the size of γ' in the interdendritic regions, and rafting behaviour. However, RR 2072 has a specific chemistry. Changes of alloy chemistry may lead to different mechanical properties. The aim of the present study was therefore to investigate the effect of minor additions on creep performance in RR2086, whose chemistry more closely resembles that of in-service materials and has also been shown to be much more stable than RR2072 in terms of TCP phase transformation [5, 6]. In this study the primary aim was therefore to investigate the effects of MC phase, rafting and porosity. TCP phase was comparatively a minor concern.

2. Experimental procedures

Rolls Royce experimental alloy RR2086 was modified with the addition of minor elements C, B and Hf. The

*Author to whom all correspondence should be addressed.

TABLE I Alloy compositions (wt%)

	Al	W	Re	Mo	Cr	Co	Hf	Nb	Ta	C	B
Base RR2086	6.2	3.35	3.4	2.7	5.2	10.0	0.10	0.8	5.5		
Modified RR2086	6.2	3.35	3.4	2.7	5.2	10.0	0.15	0.8	5.5	0.05	0.004

TABLE II Solution treatment

Alloys	Solution heat treatment	Age
RR2086	1320°C	1140°C/2 h + 870°C/16 h
Modified RR2086	1318°C	1140°C/2 h + 870°C/16 h

compositions of the base and modified alloys are given in Table I, the balance being nickel.

Both alloys were produced through SX casting. Solution heat treatment (Table II) was also required to homogenise the alloy and dissolve coarse γ' particles. To achieve the optimal homogenisation effect, the solution temperature should be as high as possible within the limit of incipient melting. Slightly lower solution temperature for the modified alloy was adjusted because of its decreased incipient melting temperature. Two ageing treatments (1140°C/2 h + 870°C/16 h) were used to promote the re-precipitation of fine uniform γ' particles. The SX casting and heat treatment were performed in Rolls-Royce plc premises.

Creep strain specimens were cut from SX bars aligned within 8° of ⟨001⟩. The specimens were tested at Rolls-Royce Derby and Bodycote Newcastle, using load control creep machines. The creep conditions were 850°C/430 MPa, 950°C/210 MPa, and 1050°C/165 MPa. The longitudinal sections of the crept specimens were examined in a Cambridge Scanning Electron Microscope 360.

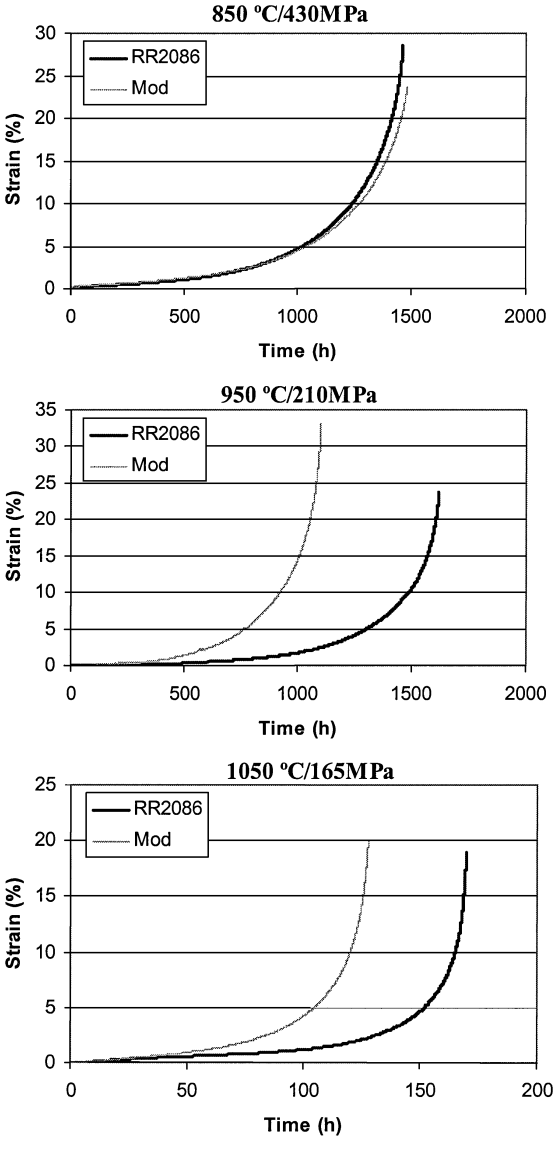

Figure 1 Creep curves at 850°C/430 MPa, 950°C/210 MPa, and 1050°C/165 MPa.

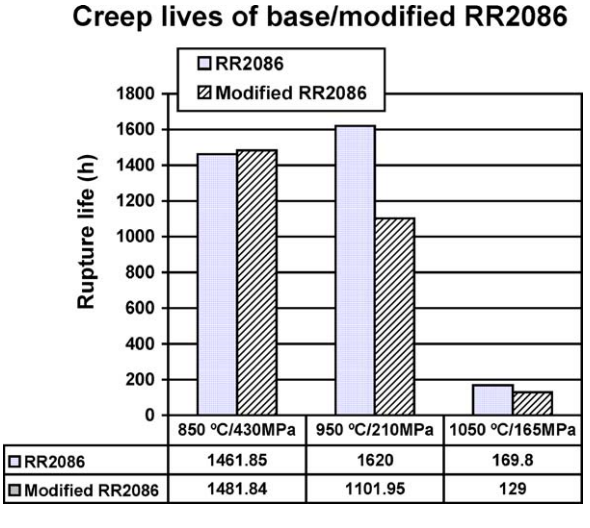

Figure 2 Creep rupture lives of the base and modified RR2086 at 850°C/430 MPa, 950°C/210 MPa and 1050°C/165 MPa conditions.

3. Results and discussion

3.1. Creep performance

Fig. 1 shows the creep curves of the base and modified RR2086 at different conditions. At 850°C/430 MPa, the two curves were very similar, particularly at the shorter times (Fig. 1a). Divergence occurred in the tertiary creep stage, the modified material having a slightly longer rupture life than the base alloy (Fig. 2). When the temperature was raised to 950 and 1050°C, however, a reversal in the performance over that at 850°C was observed. As illustrated in Fig. 1b and c, the modified RR2086 had significantly higher strain rates throughout its life than the base alloy, and consequently shorter rupture lives (Fig. 2).

3.2. Initial microstructure before creep exposure

The microstructures of the base and modified RR2086 are shown in Figs 3 and 4. The key differences observed between the two alloys were that slightly larger and more irregular γ' particles were formed eutectically with MC phase in the interdendritic regions of the modified alloy (Fig. 3), and that the porosity of the modified materials was markedly lower than the base RR2086 (Fig. 4).

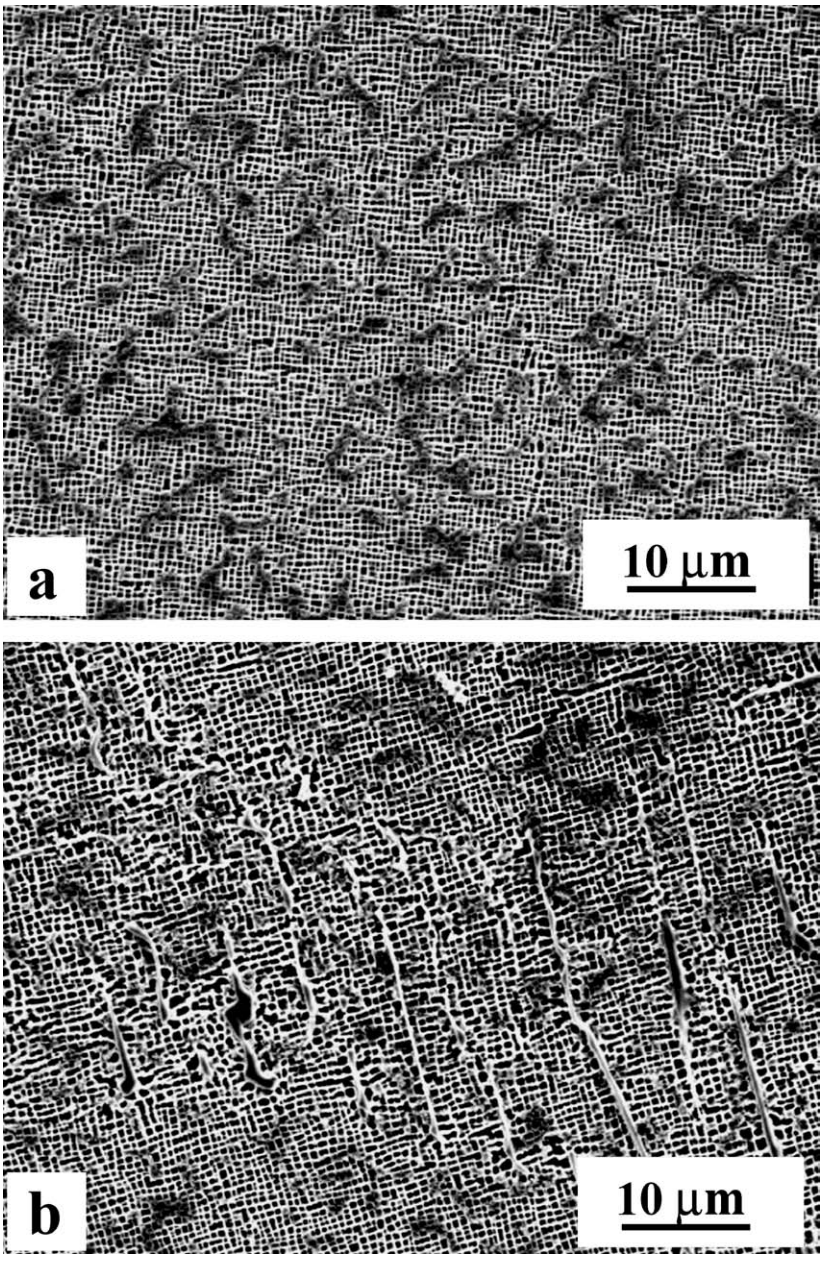

Figure 3 Microstructures of base/modified RR2086 before creep exposure: (a) Regular γ' particles are homogenously distributed in γ matrix of the base RR2086 and (b) Slightly larger and irregular γ' precipitates in an interdendrite region of the modified RR2086.

The amount of pores was determined quantitatively (Fig. 5). Using the scanning function of the specimen stage, the cross sections of alloy rod of 9 mm diameter were scanned and the sizes and positions of micropores were recorded. Three sections were examined for each alloy (i.e., six sections for the two alloys). Two of these sections are illustrated in Fig. 5, which clearly shows the reduction of porosity in the modified RR2086. Since most micropores are spherical, the volume fraction of porosity β is given by [7]

$$\beta = \frac{V_p}{V_p + V_s} \quad \text{(volume fraction)}$$
$$= \frac{A_p}{A_p + A_s} \quad \text{(area fraction)} \qquad (1)$$

where A and V refer to the area and volume of constitutes, and subscripts p and s refer to the pores and solid matrix, respectively. $A_p = \frac{\pi d^2}{4}$, where the diameter d of a pore could be measured by SEM; and $A_p + A_s = \frac{\pi 9^2}{4} = 15.9\,\text{mm}^2$. The results of β of the six sections are listed in Table III. Although scatter existed in the values of β for the same alloys, the difference between the two alloys was consistent, indicating significantly decreased porosity in the modified RR2086.

The reduction of porosity can be directly attributed to the formation of MC phase, which has a larger average metallic atom volume than the matrix [8]. MC carbides

TABLE III Fraction of porosity β in the base and modified RR2086 SX superalloys

	Base RR2086	Modified RR2086
β	0.122	0.082
	0.138	0.076
	0.124	0.060

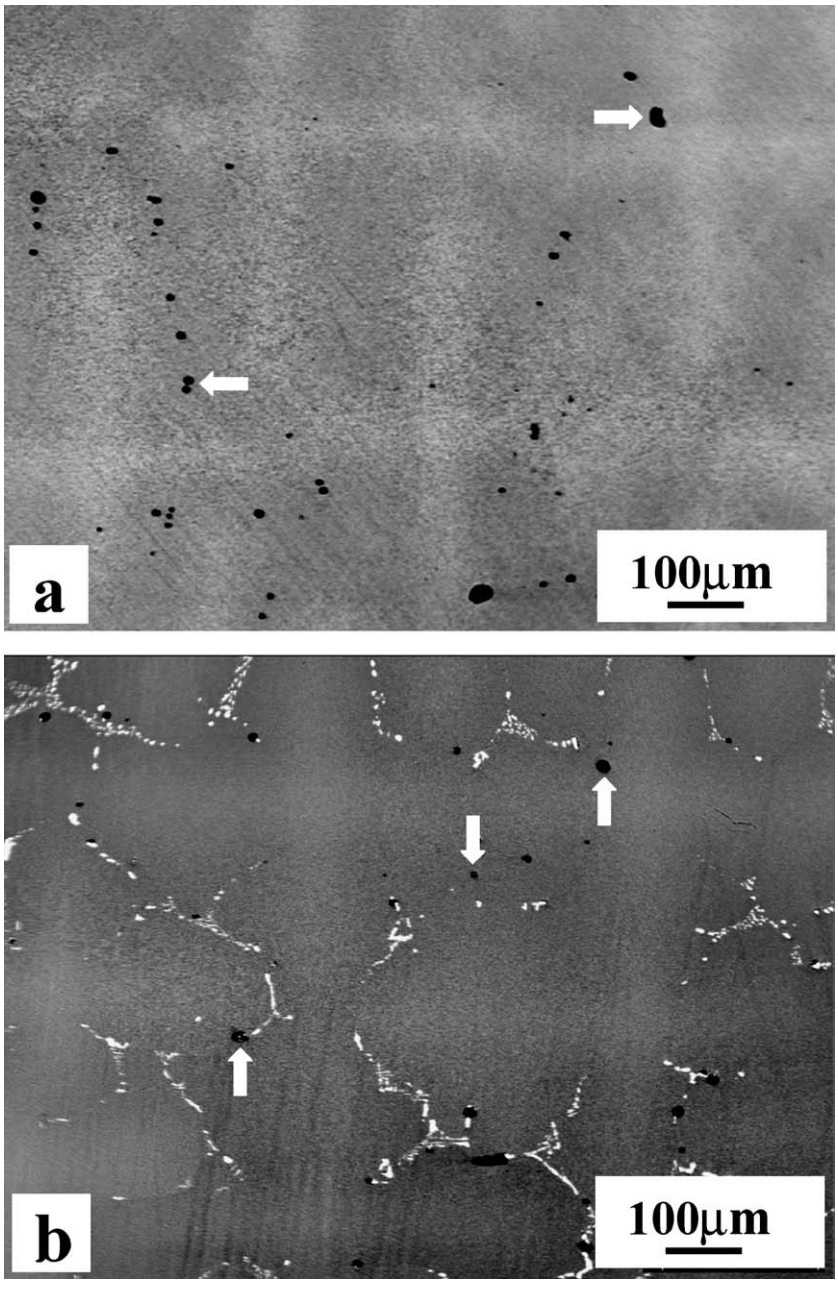

Figure 4 Porosity distribution in (a) the base and (b) modified RR2086. Some pores are indicated by arrows.

were formed in the interdendrite regions in the modified alloy, consistent with previous observations [9] and Scheil simulation using Thermo-Calc system [10] and Super-5 database. The formation of MC phase started at a temperature when about 50 wt% of solid had formed (Fig. 6). MC phase precipitation continued in the interdendritic pools after they closed up and the liquid flow was inhibited. The precipitation of MC carbides has two opposite effects on the formation of porosity. On the one hand, carbon may increase porosity because MC carbides could make bridges early [11]; on the other hand, carbides with larger average metallic atom volume may reduce microporosity due to the presence of MC carbides offsetting shrinkage associated with the final stages of solidification [12]. This bridging effect of MC carbides on microporosity, however, did not occur in the present SX superalloy, because MC carbides in the modified RR2086 were small and blocky [8], making it unlikely that they could cause early bridging. Hence, the formation of MC phase in the modified RR2086 will alleviate microshrinkage during the final stages of solidification, leading to a reduction in porosity.

3.3. Microstructure after creep exposure

A notable phenomenon in creep-tested materials is rafting (Fig. 7). It occurred at both 850 and 950°C. In the base RR2086, rafting developed throughout the specimen (Fig. 7a), but was retarded in the interdendritic space of the modified alloy (Fig. 7b and c), which contained coarse irregular precipitates prior to creep. Microcracks were initiated in these regions (Fig. 7b and c), which indicated that they were weak sites.

Another significant phenomenon is cracking from MC phase and micropores (Fig. 8). However, the cracks from MC carbides were generally much smaller than those from pores in the same creep tested samples. Eventually the small cracks were filled with materials

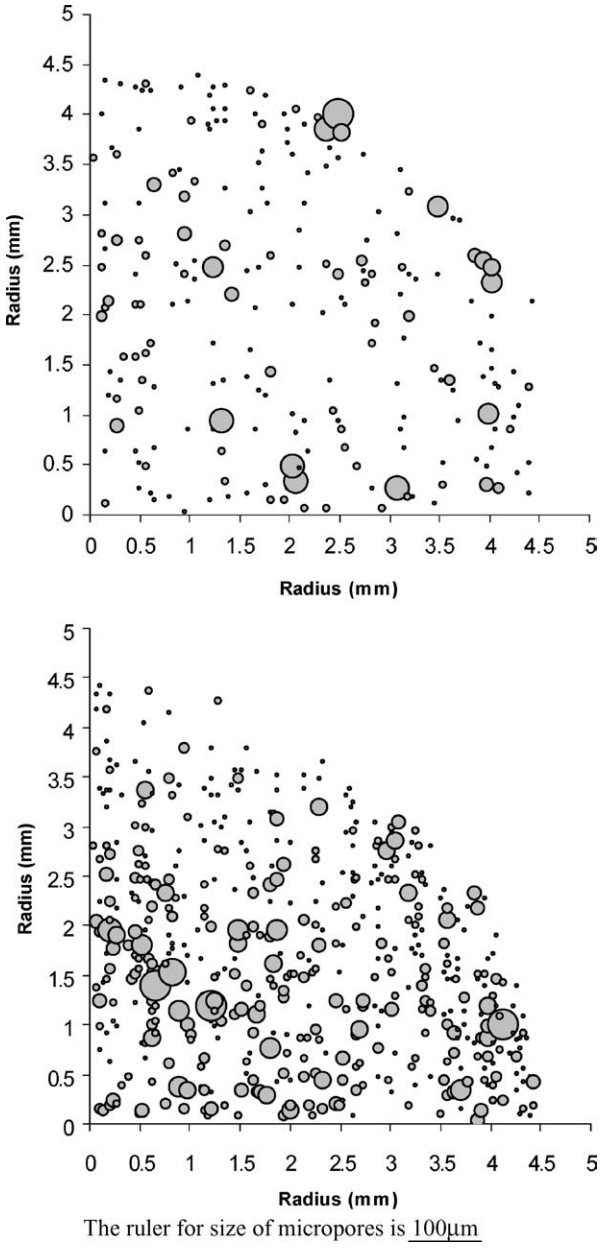

Figure 5 Microporosity distributions in (a) the modified RR2086, the number of micropores being 726, and (b) the base RR2086, the number of micropores being 352.

by diffusion during creep, and were less potentially harmful than large cracks from pores.

On the fracture surfaces, a lot of pores can be observed (Fig. 9). Although some of them might have been a result of random section on the pathway of cracking, many pores showed a flat, roughly square-shaped trace of crack propagation, which indicated that these pores were the initiation sites of cracking.

3.4. Effect of microstructure on creep performance

3.4.1. Detrimental effect

The modified RR2086 had a higher creep rate than the base alloy during the primary and secondary creep stages, particularly at higher temperatures. This phenomenon can be attributed to the weak interdendritic regions in the modified RR2086 (Fig. 3). It is known that at 700°C or higher temperatures, where thermal activation is important, the creep behaviour of superalloys with high volume fraction γ' is markedly affected by the size and shape of the strengthening particles [13, 14]. Under the employed conditions (i.e., higher temperatures and lower stresses), creep deformation proceeds by Orowan bowing of dislocations around the γ' precipitates, in which case creep strength and life decrease with the increment of γ' size [13]. The interdendritic regions that contained large irregular γ' particles were therefore weaker than the core regions. This led to high creep rates in the bulk specimen of the modified RR2086.

Another important factor is rafting. As described in Section 3.3, rafting was retarded in the eutectic regions of the modified RR2086 due to the existence of MC carbides (Fig. 7). Previous work has demonstrated the positive influence of rafting, which is attributable to the fact that dislocations can no longer climb over rafted γ' phase [15]. The beneficial effect of rafting becomes more efficient with increasing temperatures and reduced stresses, provided γ' is not cut by dislocation movement. It has been found that CMSX-2 and CMSX-3 alloys that experience this type of rafting possess

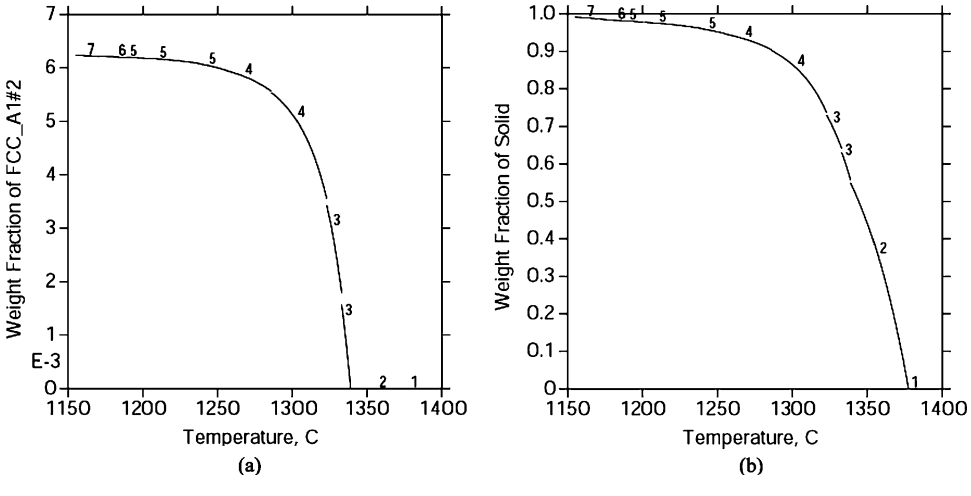

Figure 6 Scheil simulated solidification curves for the modified RR2086, using Thermo-Calc and Super5 database: (a) The solidification curve of MC phase, which indicates that MC transformation starts at 1337°C and (b) The solidification curve of all solid phases. The weight fraction of solid is about 55 wt% at 1337°C.

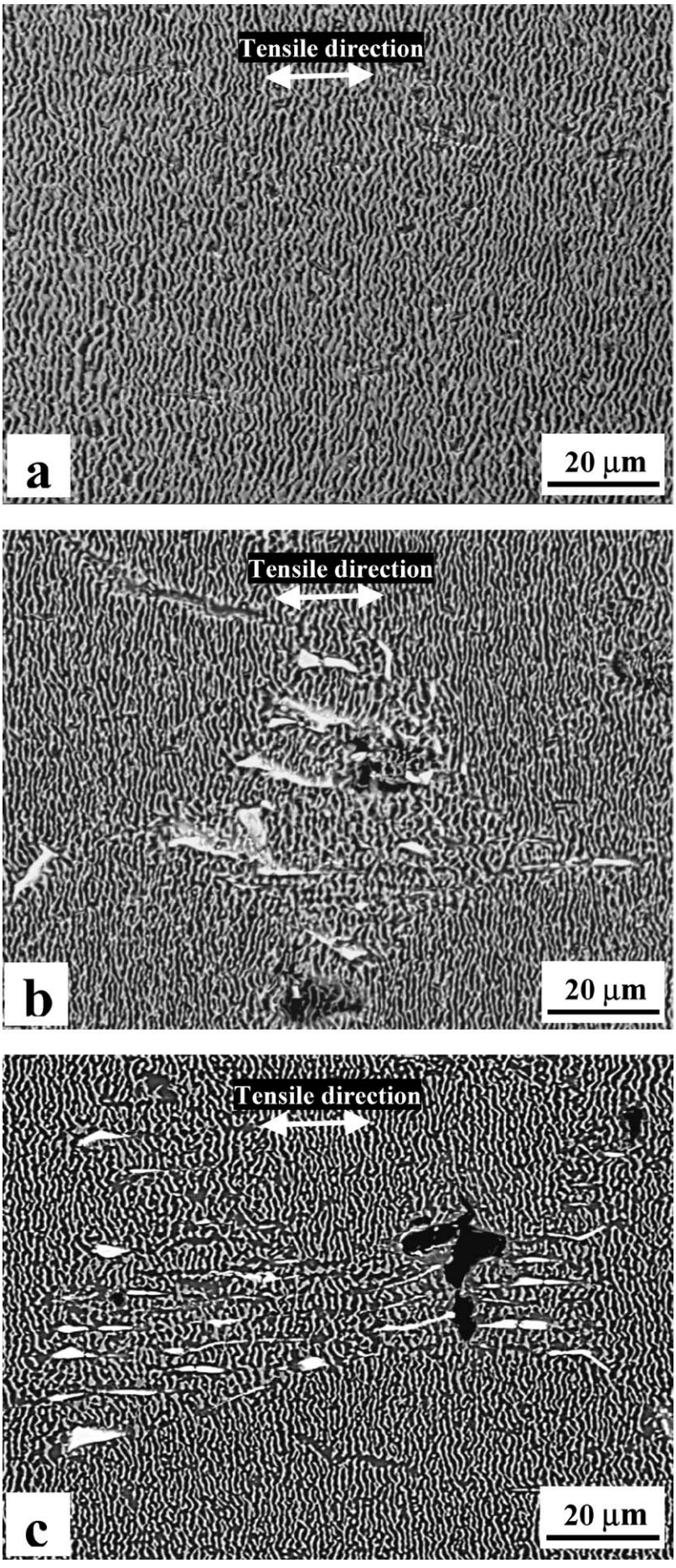

Figure 7 Rafted microstructures. (a) Base and (b) modified RR2086 at 950°C/210 MPa, (c) modified RR2086 at 850°C/430 MPa. Microcracks were initiated in the interdendritic regions of the modified alloys at both 950°C/210 MPa and 850°C/430 MPa conditions.

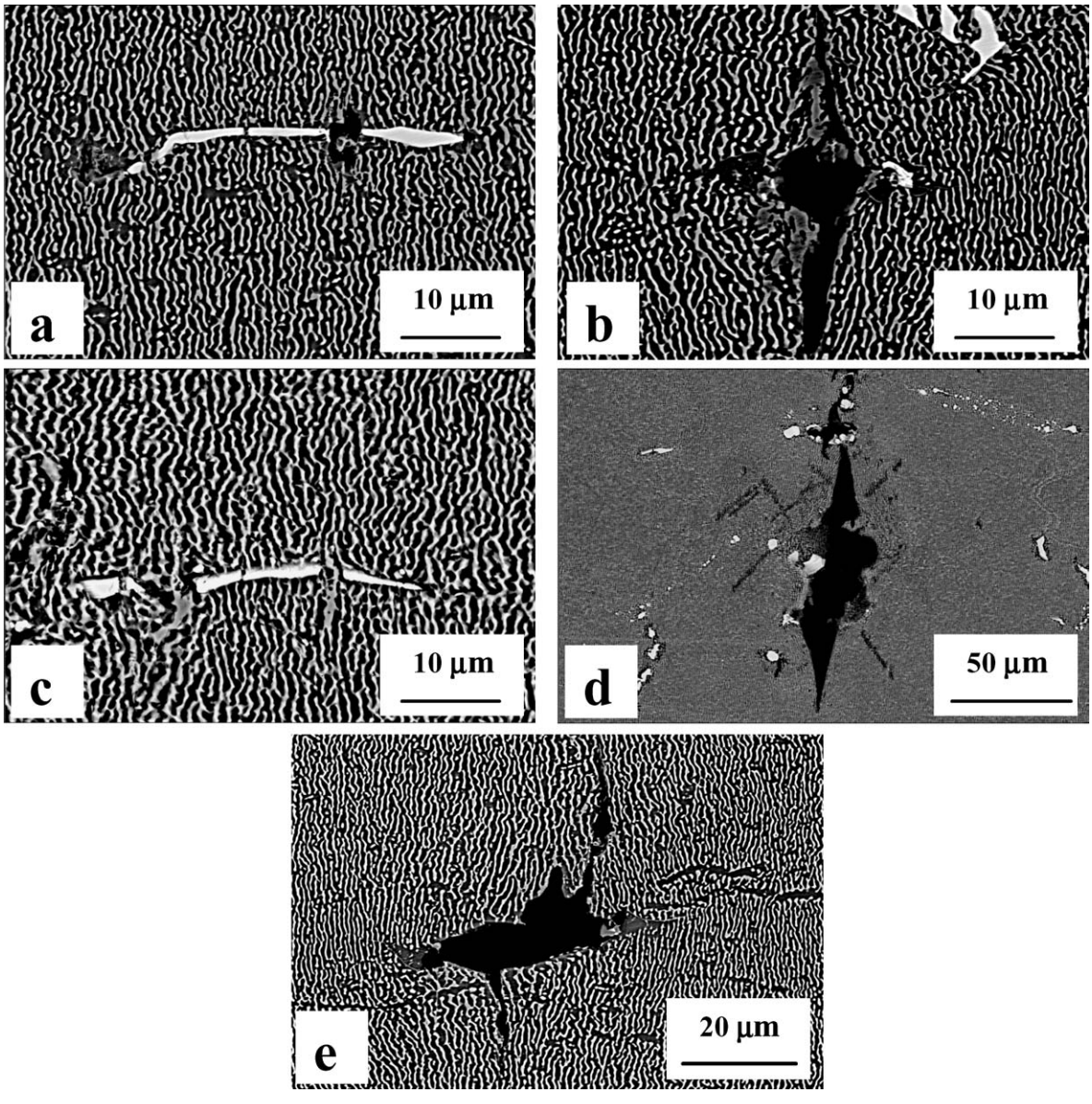

Figure 8 Cracks in creep-tested materials: (a) Small cracks were initiated from MC carbides, and (b) a large crack was initiated from a pore in the modified RR2086 at 850°C/430 MPa; (c) Small cracks were initiated from MC carbides, and (d) a large crack was initiated from a pore in the modified RR2086 at 950°C/210 MPa; (e) A large crack was initiated from a pore in the base RR2086 at 950°C/210 MPa.

remarkably enhanced rupture lives at high temperatures [16, 17]. It was postulated that the less rafted eutectic regions in the modified RR2086 were weaker than the dendrite cores at high temperatures. Consequently the modified alloy has high creep rates and short rupture lives.

Finally, MC carbides in the interdendritic regions initiated microcracks (Fig. 8), which also contributed to the weakening of the interdendritic regions in the modified RR2086.

3.4.2. Beneficial effect

At 850°C/430 MPa condition, the modified RR2086 had a longer creep life than the base alloy. The creep curves only diverged at the tertiary creep stage. The improvement of creep performance is credited to the reduction of pores in the modified RR2086. It has been shown that the primary location of creep failure is cast pores. Hence, a reduction in porosity will benefit creep behaviour at the tertiary stage. Although microcracks were also initiated from MC carbides in the modified RR2086, these cracks were much shorter and less harmful than the cavities that grew from pores. We therefore concluded that the reduction of porosity in the modified RR2086 was responsible for the improvement of creep properties.

The reduction of pores also benefited the tertiary creep performance of the modified alloy at 950°C/210 MPa and 1050°C/165 MPa. However, the detrimental influence of eutectic regions that contained large, irregular and limited rafted γ' and brittle MC phase was more dominant than the beneficial effect of porosity reduction. As a result, the modified RR2086 had shorter creep lives than the base alloy at 950 and 1050°C.

4. Summary

The microstructures that significantly affected the creep performance of the modified RR2086 were porosity reduction and weak interdendritic regions. The reduction

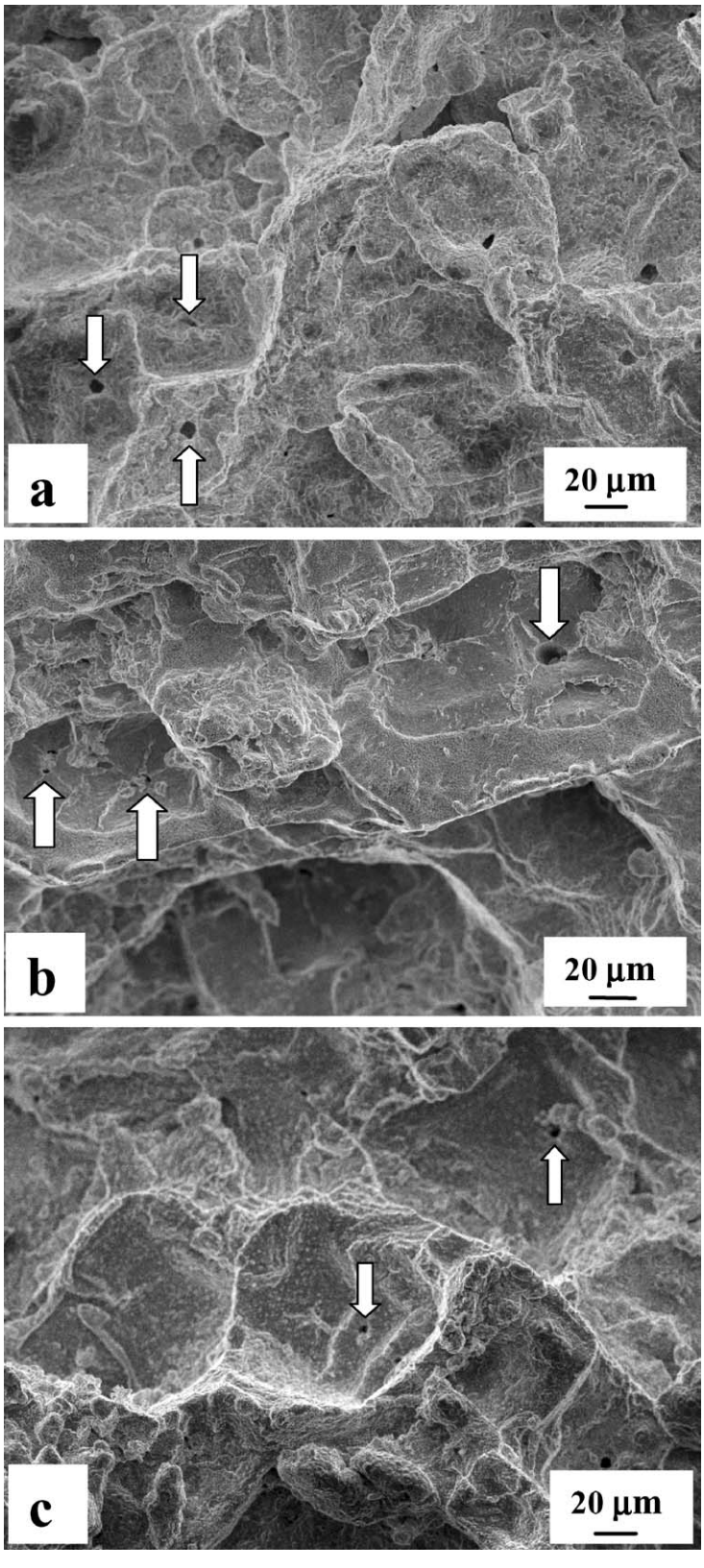

Figure 9 Creep rupture surfaces of (a) the base RR2086 at 950°C/210 MPa, (b) the modified RR2086 at 850°C/430 MPa and (c) the modified RR2086 at 950°C/210 MPa. The pores indicated by arrows showed a flat and roughly square-shaped propagation trace, which revealed that these pores were crack initiation sites.

of porosity improved creep behaviour of the modified RR2086 at the tertiary stage at lower temperatures and high stresses. The interdendritic regions that contained large, irregular and limited rafted γ' and brittle MC carbides were weak in terms of creep deformation. Their detrimental effect was more discernable at higher temperatures and lower stresses.

Acknowledgements

The authors wish to thank Rolls-Royce plc and Korea Institute of Machinery and Materials for providing the materials for this study. Thanks are also due to Dr. C.N. Jones for his helpful comments. The authors also wish to thank the Research Grants Council (Hong Kong) for its award of Grant 7345/01E.

References

1. R. F. DECKER, J. P. ROWE and J. W. FREEMAN, NACA Technical Note 4049, Washington (DC), June 1957.
2. G. L. ERICKSON, "Polyvrystalline Cast Superalloys, Metal Handbook," 10th ed. (1990) Vol. 10, p. 981.
3. C. T. SIMS, N. S. STOLOFF and W. C. HAEGEL, "Superalloys II" (John Wiley and Sons, 1987) p. 202.
4. Q. Z. CHEN, C. N. JONES and D. M. KNOWLES, *Acta Materialia*. **50** (2002) 1095.
5. Q. Z. CHEN and D. M. KNOWLES, *Metall. Mater. Trans.* A **33A** (2002) 1319.
6. Y. H. KONG and Q. Z. CHEN, *Mater. Sci. Eng.* A, under review.
7. E. E. Underwood, "Quantitative Stereology" (Edward Arnold, London, 1970) p. 23.
8. Q. Z. CHEN, C. N. JONES and D. M. KNOWLES, *Scripta Materialis* **47** (2002) 669.
9. DAVID V. NEFF, "Degassing Processes, ASM Handbook," (1996) Vol. 15, p. 457.
10. B. SUNDMAN, B. JANSSON and J. O. ANDERSSON, "The Thermo-Calc Databank System" (Calphad, 1985) Vol. 9, p. 153.
11. K. AL-JARBA and G. E. FUCKS, "Effect of Carbon Addition on Freckle Formation in Single Crystal Ni-Based Superalloys," in Proc. of Advanced Materials and Processes for Gas Turbines, Colorado, USA, 22–26 Sept. 2003.
12. Q. Z. CHEN and D. M. KNOWLES, *Mater. Sci. Tech. Lond.* **19**(4) (2003) 447.
13. F. R. N. NABARRO and H. L. DE VILLIERS, "The Physics of Creep" (Tylor and Francis, 1995) p. 194.
14. M. GELL and D. N. DUHL, in "Processing and Properties of Advanced High-Temperature Alloys," edited by S. Allen et al. (ASM, Metals Park, OH, 1986) p. 41.
15. F. R. N. NABARRO and H. L. DEE VILLIERS, "The Physics of Creep" (Taylor and Francis, 1995) p. 248.
16. T. KHAN, P. CARON, D. FOURNIER and K. HARRIS, Single Crystal Superalloys for Turbine Blades: Characterisation and Optimisation of CMSX-2 alloy, The 11th Symposium on Steel & Spatial Alloys for Aerospace, Paris, France, June 1985.
17. T. KHAN and P. CARON, Effect of Heat Treatment on the Creep Behaviour of a Ni-Base Single Crystal Superalloy, Fourth RIOS International Symposium on Metallurgy and Material Science, Office National d'Etudes et de Recherché Aerospatiales, 1983, p. 173.

Received 26 September 2003
and accepted 23 June 2004